A novel compact dual-band microstrip patch antenna achieving high gain and enhanced cross-polarization discrimination for IoT devices and next-generation wireless systems

Amul Raj C[1], *David Neels* Ponkumar D[1], and *Beulah* Jackson[1]

[1]*Department of Electronics and Communication Engineering, Vel Tech Rangarajan Dr. Sagunthala R&D Institute of Science and Technology,* Chennai-600062 India

Abstract. The escalating demand for high-performance antennas in advanced wireless systems, driven by the rapid increase of 4G/5G networks, IoT, smart cities, and automated vehicles, presents significant design challenges. Existing antenna designs often struggle to balance compactness, dual-band operation, high gain, and crucial Cross-Polarization Discrimination (XPD), which is vital for efficient Multiple-Input Multiple-Output (MIMO) systems. This paper introduces a novel compact dual-band microstrip parasitic circular patch antenna engineered to overcome these limitations. The proposed antenna, featuring a unique "flower-shaped" radiating element and utilizing a low-loss Rogers RO3003™ substrate, achieves stable dual-band operation at 2.62 GHz and 3.91 GHz. Through careful simulation and optimization, including a parametric study of substrate height, the design demonstrates excellent performance reflection coefficients (S_{11}) of -16.9 dB and -17.7 dB, VSWR values well below 2 (1.6 and 1.48), and high total gains of 5.93 dBi and 6.8 dBi at the respective bands. Crucially, the antenna exhibits outstanding XPD values of 35.44 dB at 2.62 GHz and 22.21 dB at 3.91 GHz, ensuring superior polarization purity. The findings confirm that the strategic integration of parasitic elements, optimized material selection, and precise geometry results in an antenna highly suitable for compact and reliable 4G/5G and IoT wireless communication systems, offering enhanced data capacity and reduced interference.

1. Introduction

The rapid growth of 4G/5G networks, the Internet of Things (IoT), smart cities, and automated vehicles has created a strong need for better, high-performance antennas. Modern wireless systems require antennas that are small, affordable, and able to operate in multiple frequency bands while providing high gain and excellent polarization purity [1]. These features are essential because they ensure accurate data transmission, improve signal strength, reduce interference, and support advanced technologies like Multiple-Input Multiple-Output (MIMO), which uses multiple antennas for transmitting and receiving signals to enhance overall system performance [2].

Though antenna designs have improved a lot, most current designs still have some compromises that make them less suitable for use in future wireless systems. Many conventional dual-band antennas find it hard to achieve a harmonious balance between size and good performance metrics such as gain and radiation efficiency [3]. Furthermore, a common drawback is that these antennas cannot maintain high Cross-Polarization Discrimination (XPD) level when working across multiple operating bands [4]. High XPD is very important for MIMO systems because it helps keep the two polarizations separate and independent, which increases the data capacity and reduces interference between channels [5]. If the XPD is not high enough, the advantages of using different polarizations are greatly reduced. Impacting overall system performance and reliability, particularly in dense urban environments and for mission-critical IoT applications [6]. This research specifically focuses on the 2.6 GHz band, which is an important frequency range used in 4G LTE-Advanced, 5G systems and applications such as WLAN and WiMAX due to its good balance between coverage and capacity. It also covers the 3.9 GHz band, which lies in the C-band and is commonly used for sub-6 GHz 5G services and applications like industrial IoT (IIoT) and vehicular communication.

Many studies have suggested different ways to design dual-band antennas, such as using aperture-coupled patches [7], slot-loaded patches [8] to the design. These methods do help the antenna work at two frequency bands, but they also bring some limitations. Some antennas lose gain at one or both bands because of higher losses or poor radiation. Others have good gain but low XPD, which means they don't handle polarization well. Also, antennas made to work at many bands often become larger in size, which makes them hard to use in small devices like IoT sensors and portable wireless gadgets.

This paper introduces a novel approach to address the common challenges through the design and analysis of a compact dual-band microstrip parasitic circular patch antenna. The main contributions of this works are the antenna is designed to be compact, with a ground size of

[1]Corresponding author: raj.amul1@gmail.com

54 mm × 54 mm and a main patch radius of 17.225 mm, making it well-suited for applications where space is limited, and the antenna successfully operates at two frequency bands, 2.62 GHz and 3.91 GHz, and is carefully optimized to achieve good impedance matching (S_{11} below –16 dB) and high gain values of 5.93 dBi and 6.8 dBi, respectively. Third, and lastly, the antenna has high Cross-Polarization Discrimination (XPD) values of 35.44 dB at 2.62 GHz and 22.21 dB at 3.91 GHz which is critical in enhancing capacity and reliability of a system in MIMO systems. This design employs a simple parasitic design and demonstrates that the selection of material is significant in attaining high efficiency and improved polarization performance.

2. Antenna Design and Methodology

This section presents how the dual-band microstrip parasitic patch antenna is designed, the choice of the material used, and step-by-step design procedure of the proposed antenna. The design primarily aims at maintaining the size of the antenna small and good performance at the needed frequency bands by combining established design techniques with minor modifications of the shapes.

2.1 Antenna Geometry

The given antenna is a microstrip parasitic circular patch antenna with a special flower type of radiating element like the one illustrated in Figure 1. This new form enables the antenna to attain the required dual-band applications despite being small in size. The microstrip patch antennas have low profile, can be fabricated easily and can be conformed to, and thus, they have been used in most new wireless applications [9].

The antenna is fabricated on a Low loss Roger RO3003tm substrate that is known to maintain its electrical characteristics over a large frequency range. The substrate is 3.0 relative permittivity (ε_r) and very low loss tangent (tan δ). These characteristics are used to decrease the loss of energy within the material and enhance the gain and radiation efficiency of the antenna [10].

The antenna is being carried out on a substrate of 1.4 mm thickness after careful optimization as the case will be seen in Section 2.2. The radiating element is a circular patch of radius 17.225 mm that is deposited on a square substrate plane of size 54mm x 54mm so as to have a small overall configuration.

The patch was excited by a 50-ohm inset feed line technique based upon microstrip which offers the right impedance to be excited and allow effective transfer of power [11]. The feed position and feed size are optimally set to the lowest signal reflections at the highest stability at both operating frequency ranges.

It should be mentioned that the selection of the substrate material is also significant in terms of the attainment of the good antenna performance. FR4 epoxy substrate was utilized in the first design process since it is cheap. It however gave significantly lower gain values about 1.12 dBi at the lower band and 1.56 dBi at the higher band. This was a clear indication that the increased dielectric losses in FR4 have a negative impact on the performance of the antenna [12].

The gain of the antenna increased significantly to more than 5 dBi when switched to low-loss substrate Rogers RO3003tm. This is a clear indication that the use of high-quality and low-loss materials is extremely critical in the realization of effective and high-gain performance of compact antenna designs. This significant finding indicates that it should be a total design wherein the material characteristics should be accorded the same weight as the shape and size of the antenna.

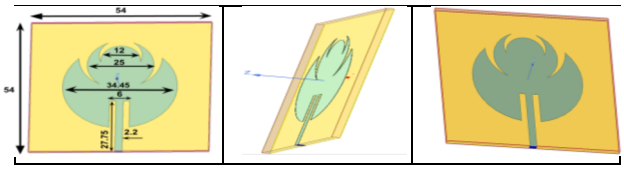

Fig.1. (a) Top view, (b) Side view, and (c) Isometric view of the proposed dual-band microstrip parasitic circular patch antenna.

2.2 Design Evolution and Dual-Band Mechanism

Its compact size also allows the antenna to give a dual-band performance, which is primarily obtained by incorporating two parasitic elements within the inner circle patch of the main patch of the antenna as seen in Figure 2(a-d). This technique is done with patch antennas and it allows the antenna to generate multiple resonant frequencies with just one radiating patch [13]. These parasitic elements have the flower shape to enhance interactions with the main patch. Not only is it appearance but it is also significant in the creation and combination of two resonant modes. One fundamental resonant frequency is supported in the main circular patch, and additional parasitic components alter the current wave and develop new resonant paths. It creates two distinct impedance dips and gives the targeted dual-band properties at 2.62 GHz and 3.91 GHz [14]. The geometry and location of these parasitic elements were optimized to a point whereby they provided robust impedance parallel and effective radiation at both target frequencies.

The ANSYS HFSS commercial electromagnetic software was used to perform the optimization process. This potent instrument allowed the comprehensive full-wave analysis and parameter sweeps in order to enhance the performance of the antenna, which is a common feature of contemporary antenna design. The parametric search of height of the substrate (h) was a critical aspect in this optimization [15]. The dielectric substrate antenna is very sensitive to the thickness of the dielectric substrate, resonant frequencies, antenna impedance bandwidth and radiations. H was varied in simulations by varying h between 0.8 mm to 2.4 mm over 10 discrete optimization steps. The steps were considered based on their influence on the S-parameters, particularly, the return loss (S_{11}) at the target frequency ranges. Out of this trial and error, it was discovered that a substrate height of 1.4 mm provides the best results, with a high radiation efficiency, dual-band impedance matching

excellently, and adequate bandwidth, and the antenna remains small. This methodological optimization is used to make sure that the completed design is resilient and meets its performance objectives in a reliable manner.

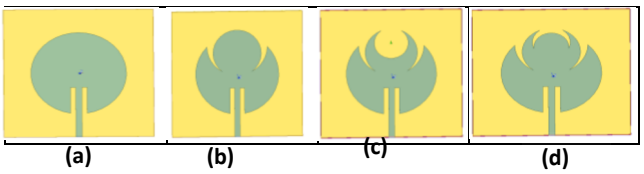

Fig. 2. Antenna evolution stages (a–d) of the proposed flower-shaped circular patch antenna, showing the step-by-step design development.

2.3 Current Distribution Characteristics

Understanding the surface current distribution on the antenna is important to understand how it resonates and how the parasitic elements help in achieving dual-band operation. Simulations performed in ANSYS HFSS provide valuable insights into the electromagnetic behavior of the antenna.

At the lower resonant frequency of 2.62 GHz, the simulated surface current distribution, as shown in Figure 3(a), exhibits strong current concentrations mainly on the parasitic elements and near their connection points with the main circular patch. This indicates that the parasitic elements are actively participating in forming the primary resonant mode at this frequency. The interaction between these parasitic structures and the main patch helps extend the effective current path, resulting in the generation of the lower resonant band. This behavior confirms that the parasitic elements play a significant role in determining the antenna's lower-band performance, rather than being purely decorative components.

In contrast, at the higher resonant frequency of 3.91 GHz, the surface current distribution, as illustrated in Figure 3(b), reveals a dominant current flow along the edges of the main circular patch, with distinct concentrations around the feed line and the boundaries of the main radiating element, and a small amount of current flowing in the first parasitic element. This pattern suggests that the main patch primarily contributes to the higher-frequency resonance, while the parasitic structure slightly alters the current path to fine-tune the impedance and enhance the radiation response.

These observations are a clear indication that the main patch and the parasitic elements at various resonant frequencies act in a complementary manner that is, the parasitic parts of an element dominate the lower band whereas the main circular patch controls the higher band. This balancing current behavior proves that the flower-shaped parasitic structure is indeed useful to facilitate compact dual-band performance without enlarging the size of the antenna.

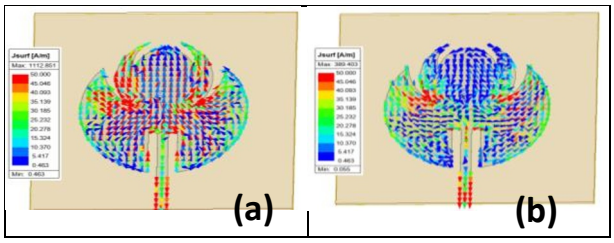

Fig.3. (a) Shows the simulated surface current at 2.62 GHz and (b) 3.91 GHz, indicating how the main and parasitic patches contribute at each frequency.

3. Results and Discussion

In this section, the detailed simulation outcomes of ANSYS HFSS of the proposed dual-band microstrip parasitic circular patch antenna are explained and discussed. Significant parameters of performance including S-parameters, VSWR, are analysed, total gain, radiation efficiency, radiation patterns, Front-to-Back Ratio (FBR), and Cross-Polarization Discrimination (XPD). These results are important for evaluating the antenna's suitability for 4G/5G and IoT applications.

3.1 S-Parameters and VSWR

The reflection coefficient (S_{11}) and Voltage Standing Wave Ratio (VSWR) are fundamental indicators that show how well the antenna matches its impedance and how efficiently it transfers power from the source to the radiating patch.

Figure 4(a) shows the simulated (S_{11}) curve of the proposed antenna across frequency. The plot clearly shows strong dual-band performance, with two deep resonance dips that are well below the -10 dB limit, which indicates good impedance matching. The first resonance occurs at 2.62 GHz, where (S_{11}) reaches -16.9 dB. The first resonance occurs at 2.62 GHz, where the (S_{11}) reaches -16.9 dB. This indicates that less than 2% of the incident power is reflected back to the source, showing very efficient power transfer to the antenna. The corresponding -10 dB bandwidth at this frequency band is around 70 MHz, which is suitable for sub-6 GHz 4G/5G applications. The second resonance is appears at 3.91 GHz with an even deeper (S_{11}) value of -17.7 dB, This signifies an excellent impedance match at the higher frequency band, reflecting minimal power. The -10 dB bandwidth at 3.91 GHz is around 100 MHz, suitable for C-band 5G and various IoT services.

Figure 4(b) shows the simulated VSWR, which directly correlates with the (S_{11}). At 2.62 GHz, the VSWR is 1.6, while at 3.91 GHz, it is 1.48. Both values are well below the desirable threshold of 2, which confirms good impedance matching and efficient power transfer in both operational bands. Such low VSWR values are important for minimizing power loss, protecting the RF circuit from damage, and ensuring reliable system performance in real-world deployments. These results clearly show that the parasitic element design and optimization process were highly effective in achieving strong dual-band performance.

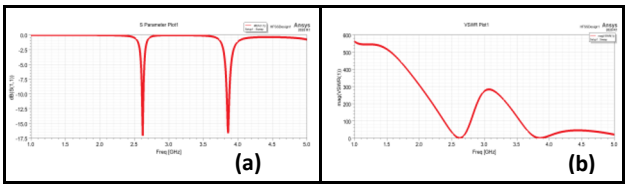

Fig. 4. (a) Simulated reflection coefficient (S_{11}) and (b) Voltage Standing Wave Ratio (VSWR) of the proposed antenna across frequency, showing excellent dual-band impedance matching.

3.2 Total Gain and Radiation Efficiency

High total gain and radiation efficiency are very important for extending communication range, improving signal strength, and ensuring energy-efficient operation in wireless systems. Figure 5(a) shows the simulated total gain of the proposed antenna across the operating frequencies. The antenna exhibits impressive gain characteristics at both resonant frequencies. A peak total gain of 5.93 dBi is achieved at 2.62 GHz, while an even higher gain of 6.8 dBi is observed at 3.91 GHz. These high gain values are impressive for a compact microstrip patch antenna, contributing significantly to enhanced signal strength, improved coverage, and reduced power requirements for transmitters.

Figure 5(b) shows the simulated radiation efficiency of the proposed antenna. The results indicate consistently high efficiency across both operating bands, mainly because of the use of the low-loss Rogers RO3003™ substrate. At 2.62 GHz, the radiation efficiency is around 80–85%, meaning most of the input power is radiated as electromagnetic waves instead of being dissipated as heat. At 3.91 GHz, the efficiency increases further to about 85–90%. These high efficiency figures underscore the effectiveness of the design in minimizing conductor losses (due to finite conductivity of copper traces) and dielectric losses (due to the substrate material). Such high efficiency is especially important for battery-powered IoT devices and for maintaining strong communication links in difficult environments. This directly translates into longer device lifespan and improved network reliability. The combination of high gain and excellent radiation efficiency clearly confirms that the antenna performs very well for a wide range of wireless applications.

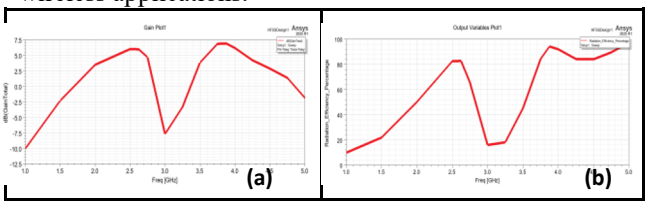

Fig. 5. (a) Simulated total gain and (b) Radiation efficiency (%) of the proposed antenna across the operating frequency range, showcasing high efficiency attributed to low-loss substrate material.

3.3 Radiation Patterns, FBR, and XPD

The radiation patterns are important in giving information on the directional characteristics of an antenna, coverage of the signal, and interference rejection. In the case of this design, the overall gain patterns as well as the co-polar/cross-polar measurements were also studied in detail.

Figure 6(a) shows that at 2.62 GHz, the simulated total gain radiation pattern in the E-plane (phi = 0°) has an extraordinarily wide main lobe, which provides it with an expansive angular coverage of the forward hemisphere. This broad-beam feature is especially beneficial in the case of applications that require large-scale coverage of the area and constant signal quality. This frequency is checked at 17.85 dB using the Front-to-Back Ratio (FBR) indicating that the backward radiation is suppressed effectively and hence, the interference that may be caused by unwanted directions is reduced to a minimum.

Figure 6(b) is then used to show the co-polarization and the cross-polarization in the E-plane. The co-polar component refers to the intended linear polarization and the cross-polar component refers to undesired orthogonal polarization components. It has been shown that the Cross-Polarization Discrimination (XPD) is excellent at boresight (0°), measuring 35.44 dB. The large XPD value indicates that the antenna is capable of maintaining purity of polarisation, which means that most of the radiated energy is contained within the desired polarisation plane, which is a critical requirement of high-performance wireless communication systems.

When the frequency is shifted to a higher value of 3.91 GHz, the radiation properties change to become more direct. The overall pattern of gain at 3.91 GHz, Figure 7(a), is in the E-plane (phi 0°), and as compared to 2.62 GHz, the main lobe is tighter and focused. Such higher directivity is useful in the concentration of power, which in this case, may prove useful in particular point-to-point or more long-range connections. The FBR of this band is 14.83 dB, which is a very good value in suppressing the backwards radiations. The co-polar and cross-polar patterns are plotted in figure 7(b) at 3.91 GHz. In this case, the XPD is observed to be 22.21 dB at boresight. Although rather lower than at 2.62 GHz, the resulting XPD of more than 20 dB is still deemed excellent in most real world uses and is a demonstration that the antenna is capable of preserving high polarization purity at the C-band.

High XPD is an essential concept whose significance can never be underestimated as far as the modern wireless communication system is concerned, which uses MIMO technology. Multiple antennas are both transmitters and receivers in MIMO systems, and polarization diversity can be used to achieve higher channel capacity and system robustness. Large XPD guarantees that the signal sent through it keeps the desired polarization states with a minimum leakage to the other polarization, thus, the orthogonality between different MIMO channels. This is essential in proper signal detection, minimize inter-channel interference and eventually maximize data throughput and reliability in congested spectral conditions. In 4G/5G networks, smart cities, and high-reliability Industrial IoT (IIoT) applications where strong communication connections and spectral efficiency are critical factors, the XPD of this antenna design is superior, which is a clear advantage.

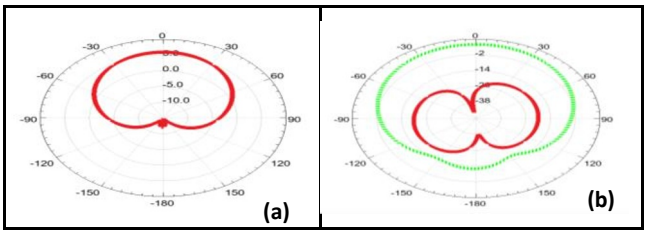

Fig. 6. Simulated radiation patterns at 2.62 GHz: (a) Total gain in the E-plane (ϕ 0°) showcasing the FBR, and (b) Co-polar and cross-polar components in the E-plane, highlighting the excellent Cross-Polarization Discrimination (XPD).

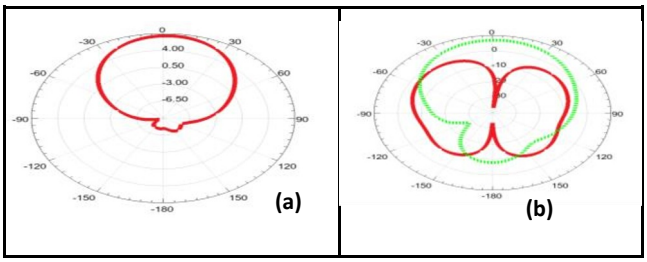

Fig. 7. Simulated radiation patterns at 3.91 GHz: (a) Total gain in the E-plane (ϕ 0°) showcasing the FBR, and (b) Co-polar and cross-polar components in the E-plane, demonstrating high XPD at the C-band.

3.4 Parametric Study of Substrate Height

The height of substrate (h) is a highly significant factor in the architecture of microstrip patch antenna. It has a direct impact on such key parameters of performance as resonant frequency, bandwidth, and impedance matching. In order to determine the optimal height at which dual bands work well, a parametric study was conducted by varying h between 0.8 mm to 2.4 mm in small steps as shown in the figure 8.

The Parametric sweep analysis (Figure 8) indicates the manner in which reflection coefficient (S_{11}) varies with variation of substrate heights. An increase in the thickness of the substrate results in an increase in the bandwidth due to increased radiation resistance. Nevertheless, an unwanted surface wave and higher-order mode may also be generated by a thick substrate, decreasing the efficiency of the antenna and altering the radiation pattern. A more narrow substrate, conversely, offers a narrower bandwidth and a greater quality factor, which restricts performance.

The outcome of the simulation is also that the resonant frequencies of both lower and upper band are highly dependent on the substrate height. With change in h, the frequency dips and their depths in the (S_{11}) curve varies, with the corresponding variations in impedance.
Upon concluding all the findings, the best height of the substrate was discovered to be 1.4 mm. The antenna performs well at this height with good resonances at 2.62 GHz and 3.91 GHz with the values of (S_{11} below -16dB for both bands) and sufficient bandwidth.

In this research the strong correlation between the height of the substrate and the performance of the antenna is evident. As such, it is necessary to maximize this parameter to have a stable, high-performance and easily fabricated design of an antenna.

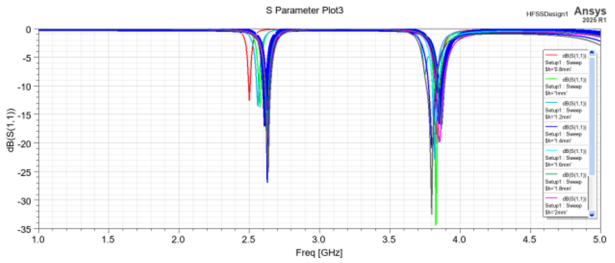

Fig. 8. Simulated reflection coefficient (S_{11}) as a function of frequency for varying substrate heights (h) ranging from 0.8 mm to 2.4 mm.

3.5 Performance Summary Table

In order to provide a clear and straightforward conception of the overall functioning of the antenna, Table I shows the important simulated parameters in both frequencies the antenna operates at 2.62 GHz and 3.91 GHz this table assists in the quick analysis of the functioning of the antenna. The table contains the key electrical and radiation features, which verify the robust and stable functioning of the suggested dual-band microstrip antenna.

Table I. Key simulated performance parameters of the proposed dual-band antenna at 2.62 GHz and 3.91 GHz.

Parameter	Value at 2.62 GHz	Value at 3.91 GHz
Ground Plane Size	54 mm × 54 mm	
Patch Radius	17 mm	
Substrate Type	Rogers RO3003™	
Substrate Height (h)	1.4 mm	
Reflection Coefficient (S_{11})	–16.9 dB	–17.7 dB
VSWR	1.6	1.48
Total Gain	5.93 dBi	6.8 dBi
Radiation Efficiency	~82%	~88%
Front-to-Back Ratio (FBR)	17.85 dB	14.83 dB
Cross-Polarization Discrimination (XPD)	35.44 dB	22.21 dB

These findings confirm that the antenna has a superior impedance matching, high gain, and purity of polarization at both frequencies, which makes it suitable in 4G/5G and internet of things wireless communication systems.

Conclusion

Through this study, we have gone through the research process, in which we have come up with a high-performance antenna, which has the ability to meet the rigid demands of wireless communication in the modern and future world. The resultant is a new compact dual band parasitic circular patch antenna that is designed on two bands but which gracefully balances size, multiple band, gain and purity of polarization trade-offs. It is a clever design in the sense that it uses radiating element in a flower shape and makes the most of superior electrical properties of Rogers RO3003tm substrate, and has risen above the limitations inherent in conventional designs.

We could demonstrate the phenomenal performance of the antenna in the selection of a prudent antenna design and optimization process, which was confirmed through intensive ANSYS HFSS simulation. It is also reliably working at two significant frequencies of 2.62 GHz and 3.91 GHz with very good impedance performance with (S_{11}) values not lower than -10 dB and VSWR values lower than 2. The reality that the antenna achieves high total gains of 5.93 dBi and 6.8 dBi is the credit of good radiation characteristics of the antenna which are further augmented by the radiation efficiencies which are consistently over 80. The Cross-Polarization Discrimination (XPD) values are also among the best values, 35.44 dB at 2.62 GHz and 22.21 dB at 3.91 GHz. This giant XPD is a necessary win, which assures signal integrity and capitalizes on the benefit of MIMO systems in dense and spectrally rich environments. The parametric experiment on substrate height brought out the fine tuning required in antenna design and the optimum of 1.4 mm thickness was selected which received this robust dual band performance.

This contribution does not only offer a good solution of compact 4G/5G and IoT application, but also the deep potential of the integration of innovative geometries and innovative material selections. The two complementary currents at the various resonant frequencies, with the parasitic elements controlling the lower band and the central patch controlling the higher, are a lovely demonstration of the complex interaction of allowing the two band operations to occur without the total size being expanded.

In the future, the research might consider how this design can be incorporated into a complete MIMO antenna array to examine the effects of mutual coupling and also optimize the spacing of elements to improve the performance of the system. Also, a discussion of reconfigurable versions of this antenna would allow the dynamic frequency tuning to fit the changing network requirements. The effective development of this small, high-performance, and polarization-pure antenna is an important movement in the search of more dependable and competent wireless communication.

References

1. C. Yoon, W.M. Seong, W.S. Kim, Compact dual-polarized quad-ridged probe antenna for spherical near-field measurement systems in 6G bands, IEEE Access, **13**, (2025).
2. M.I. Mapa, D.K. Ibarlin, E.R. Arboleda, Optimizing antenna performance: A review of multiple-input multiple-output (MIMO) antenna design techniques, Int. J. Sci. Res. Arch., **12**(2), 438–444 (2024).
3. A.K. Jassim, A compact high-gain dual-band antenna for ultrawideband applications, J. Eng. Sustain. Dev., **29**(03), (2025).
4. C. Ding, H.H. Sun, R.W. Ziolkowski, Y.J. Guo, A dual layered loop array antenna for base stations with enhanced cross-polarization discrimination, IEEE Trans. Antennas Propag., **66**(12), 6975–6985 (2018).
5. X. Tan, X. Mei, K.L. Wu, XPD enhancement of dipole antenna arrays by inducing coherent current from feeding line, IEEE Trans. Antennas Propag., **71**(5), 3950–3958 (2023).
6. S. Yamada, D. Choudhury, C. Thakkar, A. Chakrabarti, K. Dasgupta, S. Daneshgar, B. D. Horine, Cross-polarization discrimination and port-to-port isolation enhancement of dual-polarized antenna structures enabling polarization MIMO, IEEE Antennas Wireless Propag. Lett., **18**(11), 2409–2413 (2019).
7. J. M. Xie, B. Li, L. Zhu, Dual-band circular polarizers with versatile polarization conversions based on aperture-coupled patch resonators, IEEE Trans. Antennas Propag., **70**(7), 5584–5596 (2022).
8. T.H. Bui, H.T. Vu, S.X. Ta, K.K. Nguyen, C. Dao-Ngoc, N. Nguyen-Trong, Dual-band dual-polarized slotted-patch antenna for in-band full-duplex applications, IEEE Antennas Wireless Propag. Lett., **22**(6), 1286–1290 (2023).
9. K. Aafizaa, K. Uma Haimavathi, S. Saravanan, Recent innovations in microstrip patch antennas: Biomedical uses and wireless integration, Biomed. Mater. Devices, **2025**, 1–16.
10. M. El Bakkali, O. Douass, F. Rahmani, S. El Khaldi, N.A. Touhami, e-Prime – Adv. Electr. Eng., Electron. Energy.
11. S. Dase, I. Razak, Optimization of an inset-fed calculations for rectangular microstrip antenna, Comput. Sci. Inf. Technol., **4**(2), 143–148 (2023).
12. H.T. Rai, G.W. Mu, R.Q. Lu, Integrated dielectric resonator antenna to traditional antenna for better bandwidth and gain, Natl. J. Antennas Propag., **6**(2), 9–16 (2024).
13. H.T. Chou, B.A. Liu, S.C. Chen, Y.J.E. Chen, Dual-band dual-polarized microstrip patch antenna with parasitic elements for 5G antenna-in-package design at millimeter-wave frequencies, IEEE Trans. Compon. Packag. Manuf. Technol., **13**(11), 1778–1789 (2023).
14. H.H. Tran, N. Nguyen-Trong, Performance enhancement of MIMO patch antenna using parasitic elements, IEEE Access, **9**, 30011–30016 (2021).
15. S. Kong, K.M. Shum, C. Yang, L. Gao, C.H. Chan, Wide impedance-bandwidth and gain-bandwidth terahertz on-chip antenna with chip-integrated dielectric resonator, IEEE Trans. Antennas Propag., **69**(8), 4269–4278 (2021).